ISSN (Print) 1226-1750
ISSN (Online) 2233-6656
Journal of Magnetics 23(2), 293-299 (2018) https://doi.org/10.4283/JMAG.2018.23.2.293

Numerical Analysis and Experiment Study of Magnetic Fluid Boundary in Seals

Yibiao Chen[1], Decai Li[2,3]*, Yanjuan Zhang[2], and Anmin Xi[1]

[1]*School of Mechanical Engineering, University of Science and Technology Beijing, Beijing 100083, China*
[2]*Beijing Jiaotong University, Beijing 100044, China*
[3]*State Key Laboratory of Tribology, Tsinghua University, Beijing 100084, China*

(Received 15 March 2018, Received in final form 6 June 2018, Accepted 19 June 2018)

Magnetic fluid seals are widely used technical applications of magnetic fluid. This paper presents a numerical simulation model to obtain the boundary of magnetic fluid in seals. The magnetic field in the seal is solved by finite element method, and the boundary is calculated by using Navier-Stokes equations in magnetic fluid. In order to observe the surface and obtain the seal capacity, the plane magnetic fluid seal experiment is carried out. The relationship between the seal capacity and the magnetic fluid volume is presented. The seal capacity which is obtained by the theoretical analysis has well congruence with the result of the experiment. The displacement of boundary with the pressure difference is quantitatively depicted.

Keywords : magnetic fluid seal, numerical analysis, experiment study, seal capacity, boundary

1. Introduction

Magnetic fluid is a ferromagnetic material in liquid state, which can be controlled by magnetic field. Magnetic fluid seals are the best known applications of magnetic fluid. Magnetic fluid seals have been widely used in shipbuilding industry, military project, chemical engineering and other industries [1-3].

A number of studies have been conducted on numerical analysis of magnetic fluid seals. In previous studies, the boundary of magnetic fluid is tightly related to the pressure difference. And the seal capacity is enhanced with the increase of the fluid volume. Potoczny *et al.* [4] conducted several experiments to obtain the influence of magnetic fluid volume onto the burst pressure in the seal. Park *et al.* [5] presented a numerical algorithm to calculate the boundary surface in the magnetic fluid seal. Radionov *et al.* [6] developed a mathematical model for analyzing the magnetic field in the seal and calculated the distribution of the magnetic force of magnetic fluid. Jibin *et al.* [7-9] used numerical computations to study the performance of magnetic fluid seal influenced by other parameters. The magnetic fluid seals with pressure control system was designed to against high-pressure differential. Szczech *et al.* [10, 11] conducted the critical pressure experiments to research the pressure distribution mechanism among stages. The pressure in the region between two adjacent stages was measured. And the relationship between the critical pressure and temperature was obtained through the experiment method. Zhang *et al.* [12] conducted the research on the static pressure in multi-stage magnetic fluid seals. The magnetization of the fluid was studied by experiment method, the Boltzmann fitting and the Langevin fitting. Chen *et al.* [13] carried out numerical study on the key parameters of the seal with large gap by finite element method.

Recent studies lack of numerical simulation and experiment study on the boundary of magnetic fluid in seals. And there was little research on the deformation of magnetic fluid due to the pressure difference. In this paper, we describe the equation for modelling the boundary of the fluid in seals. The relationship between fluid surface deformation and pressure difference is quantitatively depicted. The burst pressure of a single tooth is computed. Besides, the plane magnetic fluid seal experiment is carried out in order to observe the surface and obtain the seal capacity experimentally. It is found that the experimental results are consistent with the analysis results.

2. Mathematical Model

In order to analyze magnetic fluid seal, the magnetic

*Corresponding author: Tel: +86-10-5168-5265
Fax: +86-10-5168-4006, e-mail: lidecai@mail.tsinghua.edu.cn

field equations and hydrodynamic equations should be solved separately, such as Maxwell equations and Navier-Stokes equations. The coupling calculation of flow field and magnetic field is difficult since two fields influence each other.

The magnetic field in the seal can be solved by using Maxwell equations. The equations are represented as follows,

$$\nabla \times \boldsymbol{H} = 0 \tag{1}$$

$$\nabla \cdot \boldsymbol{B} = 0 \tag{2}$$

where $\boldsymbol{H}$ and $\boldsymbol{B}$ are the magnetic field strength and magnetic induction, respectively. The dependence of $\boldsymbol{H}$ and $\boldsymbol{B}$ is described by $\boldsymbol{B} = \mu_0(\boldsymbol{H} + \boldsymbol{M})$, where $\boldsymbol{M}$ denotes the magnetization and μ_0 is the permeability constant. The distribution of magnetic induction $\boldsymbol{B}$ is solved by using the finite element method.

The system is considered to be in steady state, and the magnetic fluid inviscid, incompressible and homogeneous. Based on Navier-Stokes equations, the pressure inside the fluid is given as follows [14],

$$p_i + \rho g h - \mu_0 \int \boldsymbol{M} \mathrm{d}\boldsymbol{H} = c \tag{3}$$

where, p_i, ρ, g, h and c are the pressure inside the fluid, fluid density, gravitational constant, height of the fluid and the constant in the fluid, respectively. Since the direction of the magnetization is parallel to the direction of magnetic field strength, equation (3) can be expressed as follows,

$$p_i + \rho g h - \mu_0 \int M \mathrm{d}H = c \tag{4}$$

where M and H are modules of magnetization and magnetic field strength, respectively.

At the two sides of the interface between the air and the magnetic fluid, the normal component of the magnetic induction intensity and the tangential component of the magnetic field strength are continuous. When the influence of gas-liquid surface tension force is neglected, the relation between the pressure inside and outside the magnetic fluid is given as follows [14],

$$p_i + \frac{1}{2}\mu_0 M_n^2 = p_o \tag{5}$$

where p_o and M_n are the pressure outside the fluid and the normal component of the magnetization, respectively.

On the surface of magnetic fluid, equation (4) and equation (5) must be satisfied simultaneously. Substituting equation (4) into equation (5), we obtain equation (6) as follows.

$$c = p_o + \rho g h - \mu_0 \int M \mathrm{d}H - \frac{1}{2}\mu_0 M_n^2 \tag{6}$$

From equation (6), we can know that the shape of magnetic fluid under the pole tooth is related to the pressure outside the fluid, magnetization characteristic of magnetic fluid and magnetic field strength. The pressure which caused by magnetic field is calculated by the integral calculation according to magnetization curve of magnetic fluid.

A computing model of the magnetic fluid seal is shown in Fig. 1. As seen in Fig. 1, a magnetic fluid seal consists of a shaft, a magnet, two pole shoes and magnetic fluid. Figure 2 is the model for the region under the sixth tooth on the right pole shoe. The pressure at the left side of magnetic fluid is higher than it at the right side.

The value of c in equation (6) is constant on the fluid boundary. Hence, the boundary coincides with the contours of c. The boundary is determined by the magnetic fluid volume. In order to obtain the boundary of magnetic fluid under the pole tooth and seal capacity of a single tooth, the iterative computation is as follows:

1. Import the pressures at both sides of the tooth and the fluid volume V_{im};

2. Calculate the magnetostatic field in the magnetic fluid seal in Fig. 1 by finite element method;

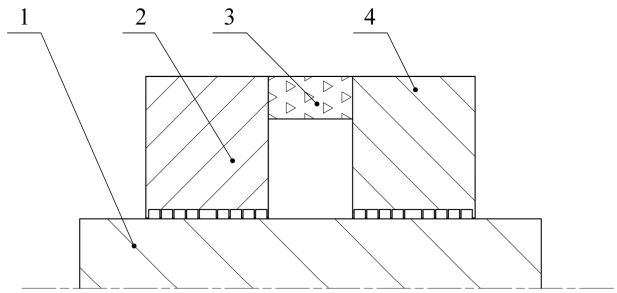

Fig. 1. The calculation model of the magnetic fluid seal: 1- shaft, 2- left pole shoe, 3- magnet, 4- right pole shoe.

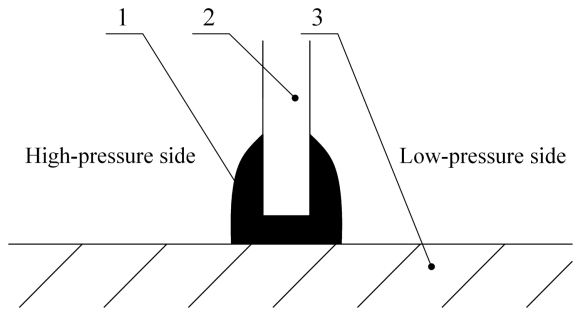

Fig. 2. The region under the pole tooth: 1- magnetic fluid, 2- pole tooth, 3- shaft.

3. Compute the ρgh, $\mu_0 \int M\mathrm{d}H$ and $\frac{1}{2}\mu_0 M_n^2$ in the region under the tooth as shown in Fig. 2;

4. Add up four values at the right side of the equation (6), obtain distribution of c at both sides of the tooth;

5. Select an appropriate value of c, calculate the contours of the value at both sides of the tooth, respectively;

6. Calculate the area of the region surrounded two contours, shaft and the tooth, obtain the volume, V_{ca}, under the single tooth with the value of c;

7. Compare V_{ca} with V_{im}. If $V_{ca} > V_{im}$, increase the value of c; if not, decrease the value; Return to step 5, and recalculate the boundary until the relative error of two volumes is less than 1×10^{-3};

8. Return to step 2, and recalculate the magnetostatic field until it is convergent.

The boundary of magnetic fluid changes while pressure difference increases. The iterative computation will fail to get a result if pressure difference is higher than the burst pressure. The seal leakage occurs while the magnetic fluid in the gap is blown out. In this way, the seal capacity of a single tooth can be computed.

3. Experimental Methods

In this section, the experimental device, experimental procedure and measuring method are described.

As shown in Fig. 3, the experimental device consists of the plane magnetic fluid seal, pressure sensors, a pressure reducing valve and a data acquisition system, etc. During testing the seal, air is delivered from a high pressure gas cylinder. The pressure is regulated by the pressure reducing valve which is made by FEFA. The pressures of the air on both sides of the pole tooth are measured using two pressure sensors, of which the measuring ranges are from 0 to 40 kPa. The deformation of magnetic fluid with

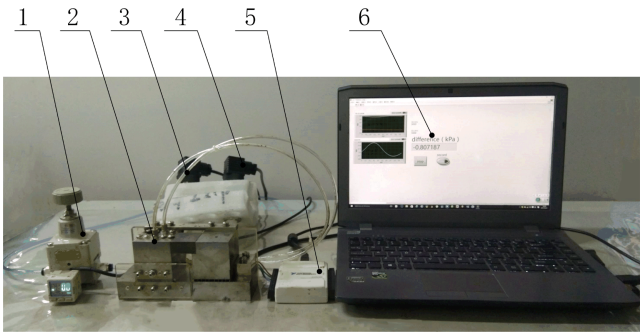

Fig. 3. (Color online) The experimental device of magnetic fluid seal: 1- pressure reducing valve, 2- magnetic fluid seal, 3- high-pressure sensor, 4- low-pressure sensor, 5- measurement card, 6- computer.

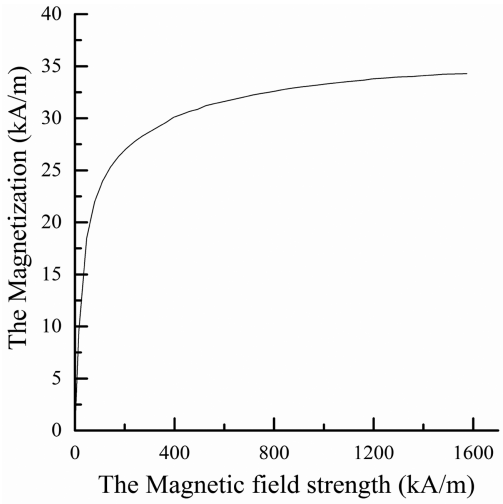

Fig. 4. The magnetization curve of the magnetic fluid.

the increase of the pressure difference is recorded by a camera. The camera can record the image information within 0.05 mm with a macro lens. In order to increase coloring differences between the boundary and the background, a light is placed behind the plane seal.

The pressure signals are sent to the NI USB-6009 eight-channel measurement card of National Instruments, which cooperates with the computer by making use of LabVIEW software.

The magnetic fluid seal consists of a permanent magnet, pole shoes, a shaft, and magnetic fluid. The pole shoes are made of 2Cr13 with teeth which gather magnetic field lines. The magnet is made of NdFeB with the grade N35. The shaft is made of 2Cr13, and the width of the gap between the shaft and tooth is 0.35 mm. The magnetic fluid used in the experiment is kerosene based with the magnetization curve shown in Fig. 4, viscosity of 6.5 mPa·s and density of 1.22 g/cm^3.

4. Result and Discussion

Figure 5 shows the distribution of B in the magnetic fluid seal and the region under the tooth (the rectangle in Fig. 5(a)), where B presents the module of magnetic induction. It is clear that the maximum magnetic induction is in the pole tooth which equals to 1.8 T. Figure 6 shows the magnetic field lines in the seal. From Fig. 6, we can see that magnetic field lines are gathered in the tooth. The magnetic force, which is caused by the gradient of magnetic induction, immobilizes the magnetic fluid in the clearance.

The surfaces of magnetic fluid obtained through simulation and experiment are shown in Fig. 7. Compared

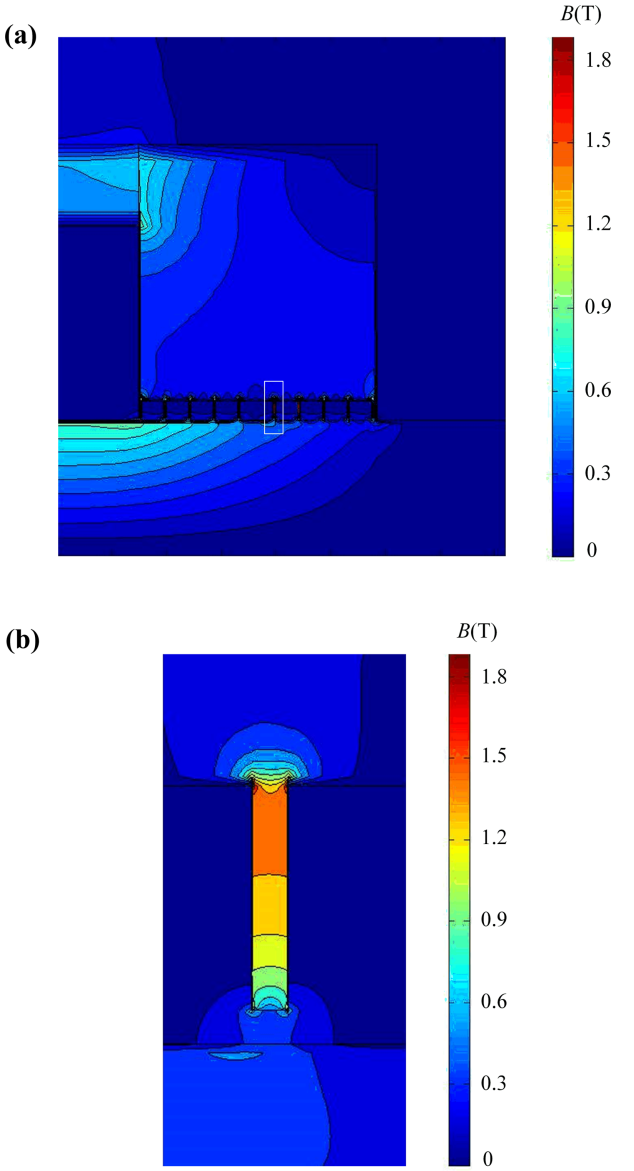

Fig. 5. (Color online) Distribution of magnetic induction in (a) the magnetic fluid seal and (b) the region under the tooth.

with the experiment result, the boundary of the fluid obtained through simulation has the bigger contact angle, since surface tension is neglected in the simulation. In the further research, the influence of surface tension will be taken into account in order to obtain more accurate estimation.

The boundary of magnetic fluid is influenced by the pressure difference and the volume of magnetic fluid. In order to quantify the displacement of the boundary, we calculate the coordinate of intersection points of the shaft and the boundary under different pressure differences. Points A_h and A_l in Fig. 7 present the intersection points at the high-pressure side and low-pressure side, respectively. Figure 8 shows that the displacement of magnetic fluid boundary has great linear with the pressure differ-

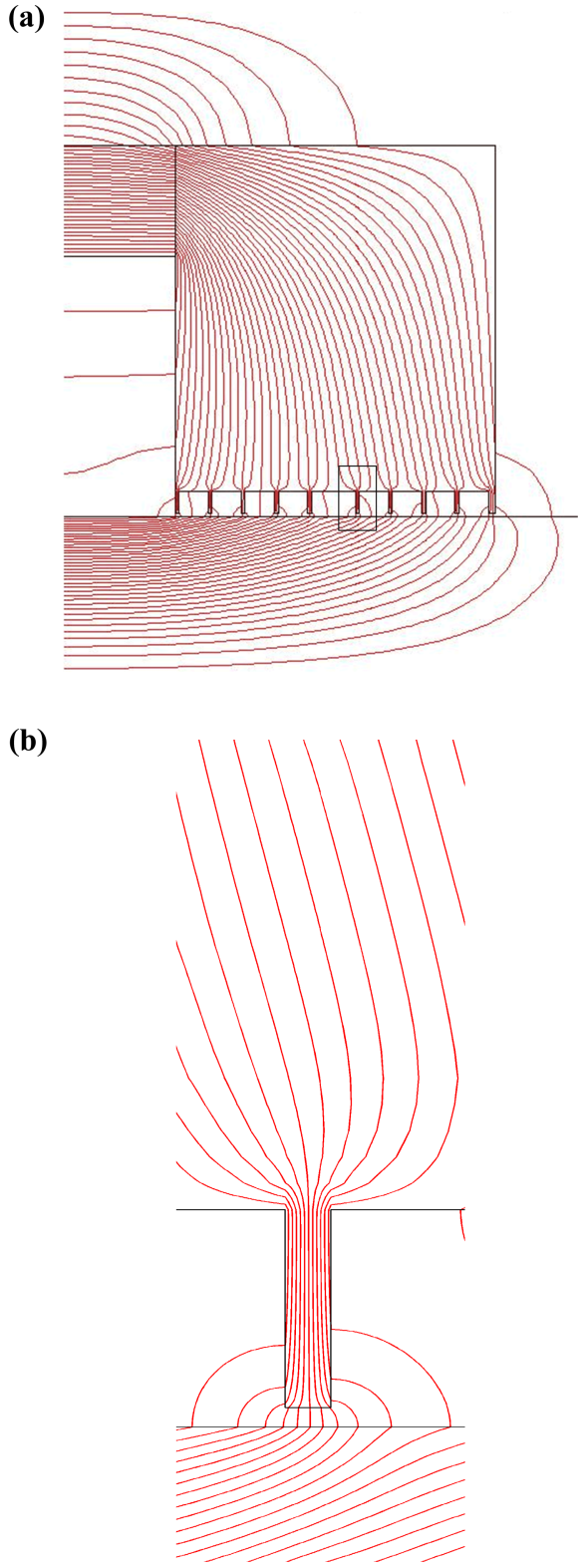

Fig. 6. (Color online) Distribution of magnetic field lines in (a) the magnetic fluid seal and (b) the region under the tooth.

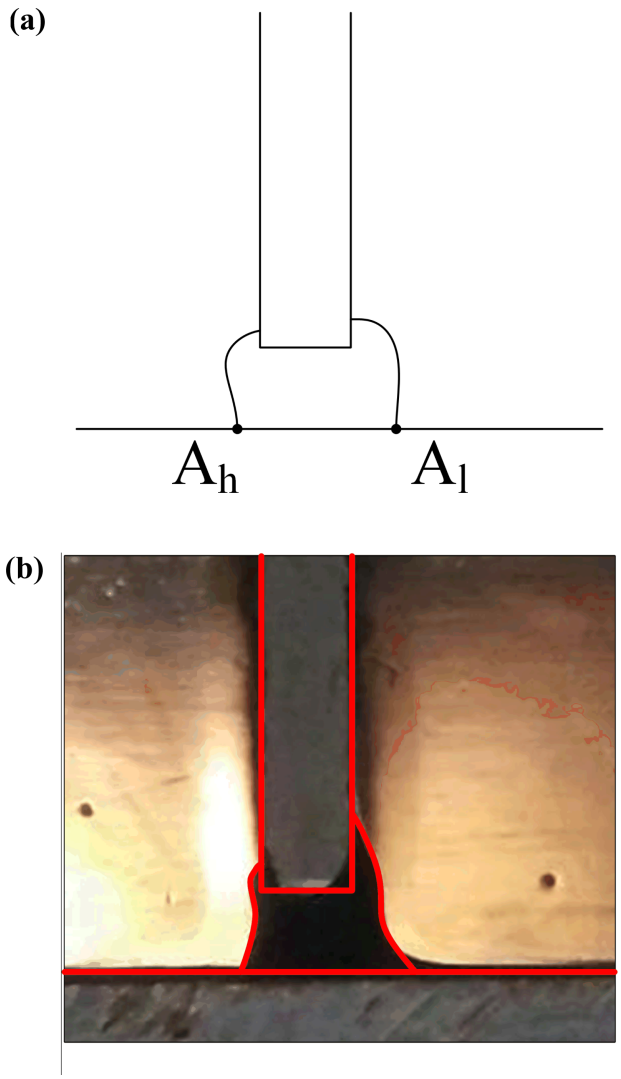

Fig. 7. (Color online) Surfaces of magnetic fluid obtained through (a) simulation and (b) experiment.

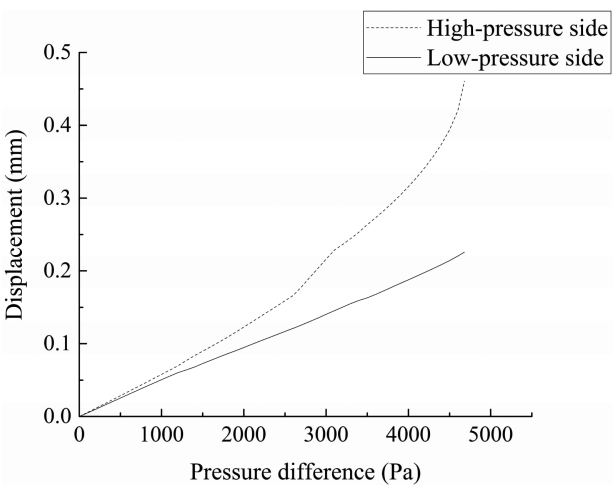

Fig. 8. The displacement of magnetic fluid boundary.

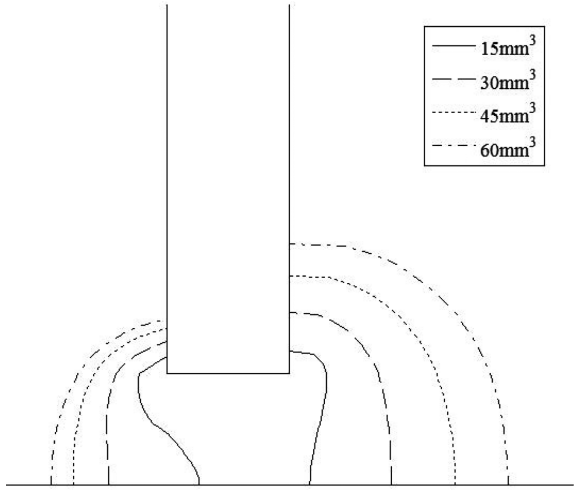

Fig. 9. Surfaces of magnetic fluid with different volumes.

ence. The displacement which takes place at the high-pressure side is more than double that at the low-pressure side. Under the burst pressure, the intersection point A_h moves 0.46 mm while A_l moves 0.22 mm.

The volume of magnetic fluid also has an impact on the boundary of magnetic fluid. Figure 9 shows the boundary with different volumes under the pressure difference of 2 kPa. The distance between the intersection point and pole tooth increases with the increase of the volume. Compared with the surface at the high-pressure side, the surface at the low-pressure side has more obvious difference due to the volume.

The magnetic fluid is blown out from the seal in the axial direction when the pressure difference exceeds the burst pressure. The seal leakage occurs in the weakest place of the magnetic fluid ring. The burst pressure of magnetic fluid seal is related to the mechanical structure

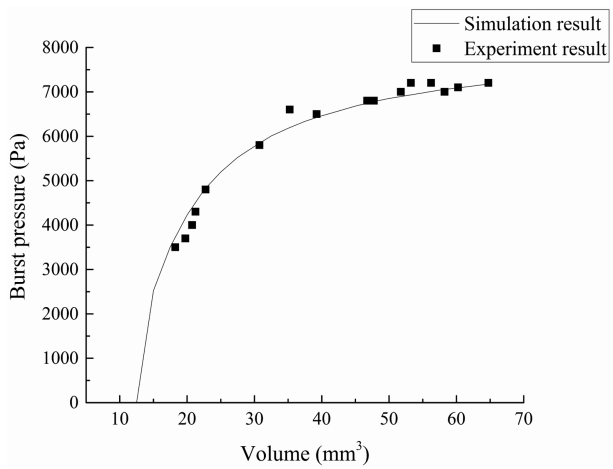

Fig. 10. The relationship between burst pressure and the volume of the magnetic fluid.

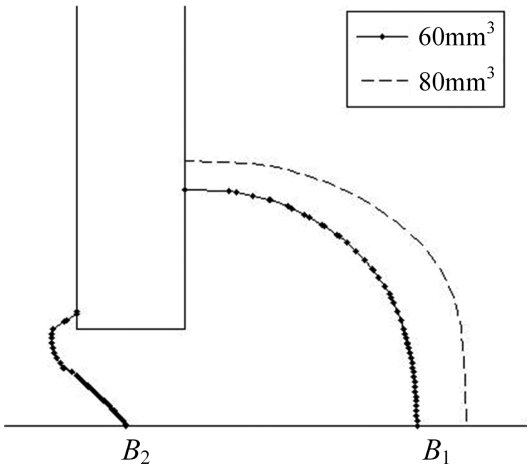

Fig. 11. Surfaces of magnetic fluid with different volumes under the burst pressures.

of the seal, the material performance of parts and the volume of the magnetic fluid. In the paper, we investigate the relationship between the burst pressure and volume of the magnetic fluid.

Figure 10 presents the diagram of the volume of the magnetic fluid to the burst pressure. It is obvious that the burst pressure increases with increasing volume of the magnetic fluid. The growth rate of burst pressure slows down when volume exceeds 30 mm^3.

Figure 11 shows surfaces of magnetic fluid with different volumes under the burst pressures. In Fig. 11, the solid line with dots refers to the boundary of magnetic fluid with the volume of 60 mm^3, and the dashed line refers to that with the volume of 80 mm^3. The burst pressures of two volumes are 7085 Pa and 7370 Pa, respectively. The burst pressure increases 4 % while the fluid volume increases 33 %.

It is well known that the seal capacity of magnetic fluid seal can be approximately expressed as follows [14],

$$\Delta p = \int_{B_1}^{B_2} M \mathrm{d}B \tag{7}$$

where, B_1 and B_2 are the magnetic inductions at the intersection points of the shaft and fluid boundary at the low-pressure and high-pressure side under the burst pressure, respectively. The positions of the intersection points are shown in Fig. 11. And Δp is the burst pressure of the seal. We can assume that the fluid is saturated due to the high magnetic field intensity in the computational domain. Hence equation (7) can be expressed as follows,

$$\Delta p = M_s \cdot (B_2 - B_1) \tag{8}$$

where, M_s is the saturation magnetization of magnetic fluid. It can be seen from the equation (8) that the burst pressure is associated with the B_1 and B_2.

As shown in Fig. 11, boundary of magnetic fluid at the side of high pressure has no obvious variation with the increase of volume, so B_2 with different volumes almost remains unchanged. The boundary shifting takes place at the side of low pressure. In the region of the boundary, gradient of magnetic induction in the region of the boundary is much smaller than that in the clearance. Therefore, the difference between the two magnetic inductions of two boundaries at low-pressure side is less than 0.02 T. According to equation (8), there is little difference between two burst pressures of two volumes. Hence, there is little beneficial effect from the increase of the magnetic fluid volume on improvement of seal capacity when the fluid is sufficient.

In Fig. 10, the curve and points refer to results of simulation and experiment, respectively. The maximum error between the experimental and theory value of the burst pressure is 450 Pa. The relative error is 6 %. The seal capacity obtained by the theoretical analysis has well congruence with the result of the experiment. The error is caused by the following reasons. The clearance size exists errors due to an inaccuracy in producing and assembling elements of experimental device, which decreases the gradient of magnetic induction and reduces the seal capacity. The material properties, such as the permeability of shaft, also lead to an inaccurate result.

5. Conclusion

In the paper, the seal capacity of magnetic fluid seal and surface of the magnetic fluid have been investigated through experimental and simulation method.

Based on the obtained results, the following conclusions and recommendations can be suggested:

1. The boundary of the magnetic fluid has been obtained through experimental and simulation method. The displacement of magnetic fluid boundary is related to pressure difference. The magnetic fluid is blown out from the seal while the pressure difference exceeds the burst pressure.

2. The burst pressure of the magnetic fluid seal increases with increasing volume of the magnetic fluid. When the volume increases to a critical value, the burst pressure remains unchanged. In a practical application, controlling the volume of magnetic fluid precisely generates cost savings.

3. There are deviations between the calculated result and experimental result, which may be caused by the errors in the process and assembly, differences in the experimental and calculated material properties, simpli-

fication in the calculation process. These problems will be overcome in subsequent studies, which will lead to better agreement between the experimental and computed results.

Acknowledgement

This work was supported by the Program for Changjiang Scholars and Innovative Research Team (grant no. IRT17R07), the program of main shaft sealing used ferrofluids (grant no. KM16GY500010) and the Program of Graduate innovation of Beijing Jiaotong University (Grant no. 2017YJS163).

References

[1] L. Matuszewski and Z. Szydło, Pol. Marit. Res. **15**, 49 (2008).
[2] Y. Mitamura, S. Takahashi, S. Amari, E. Okamoto, S. Murabayashi, and I. Nishimura, Journal of Artificial Organs the Official Journal of the Japanese Society for Artificial Organs **14**, 23 (2011).
[3] C. Ming, Chin. J. Mech. Eng.-En. **25**, 706 (2012).
[4] M. Potoczny and B. Zachara, Key Engineering Materials **490**, 119 (2012).
[5] G. S. Park, D. H. Kim, S. Y. Hahn, and K. S. Lee, IEEE Trans. Magn. Magn. **30**, 3351 (1994).
[6] A. Radionov, A. Podoltsev, and A. Zahorulko, Procedia Engineering **39**, 327 (2012).
[7] Z. Meng, J. Zou, and J. Hu, J. Magn. Magn. Mater. **303**, e428 (2006).
[8] J. Zou, X. Li, Y. Lu, and J. Hu, J. Magn. Magn. Mater. **252**, 321 (2002).
[9] J. Zou, J. Zou, and J. Hu, IEEE Trans. Magn. **39**, 2651 (2003).
[10] M. Szczech and W. Horak, IEEE Trans. Magn. 1 (2017).
[11] M. Szczech, IEEE Trans. Magn. 1 (2018).
[12] Y. Zhang, Y. Chen, D. Li, Z. Yang, and Y. Yang, IEEE Trans. Magn. 1 (2017).
[13] F. Chen, X. Yang, S. Gao, Y. Chen, F. Chen, X. Yang, S. Gao, and Y. Chen, Int. J. Appl. Electrom. Mech. **55**, 1 (2017).
[14] Rosensweig, RonaldE, Ferrohydrodynamics, Cambridge University Pre, 151 (1985).